Inflammation and immunomodulation in uveal melanoma
Ly, L.V.

Citation
Ly, L. V. (2011, April 12). *Inflammation and immunomodulation in uveal melanoma*. Retrieved from https://hdl.handle.net/1887/16710

Version:	Corrected Publisher's Version
License:	[Licence agreement concerning inclusion of doctoral thesis in the Institutional Repository of the University of Leiden](#)
Downloaded from:	https://hdl.handle.net/1887/16710

Chapter 8

Peptide vaccination after T-cell transfer causes massive clonal expansion, tumor eradication, and manageable cytokine storm

Long V. Ly[1], Marjolein Sluijter[2], Mieke Versluis[1], Gregorius P.M. Luyten[1], Sjoerd H. van der Burg[2], Cornelis J.M. Melief[3], Martine J. Jager[1], and Thorbald van Hall[2]

Departments of Ophthalmology[1], Clinical Oncology[2], and Immunohematology and Blood Transfusion[3], Leiden University Medical Center, Leiden, the Netherlands

Abstract

Adoptive T-cell transfer (ACT) is successfully applied as a cancer treatment that is based on the activation and effector functions of tumor-specific T cells. Here, we present results from a mouse model in which ACT is combined with a long peptide–based vaccine comprising gp100 T-cell epitopes. Transferred CD8+ T cells expanded up to 1,000-fold after peptide vaccination, leading to a 3-fold increase in white blood cell count and a very high frequency in the generation of antigen-specific memory T cells, the generation of which tended to correlate with effective antitumor responses. An enormous pool of effector T cells spread widely to different tissues, including the skin and the immune-privileged eye, where they mediate tumor eradication. Importantly, these striking T-cell dynamics occurred in immunocompetent mice without prior hematologic conditioning. Continued activation of the specific T-cell pool by vaccination led to strong T-cell–mediated cytokine storm and lethality due to multi-organ failure. However, this immunopathology could be prevented by controlling the rapid biodistribution of the peptide or by using a weakly agonistic peptide. Together, these results identify a peptide vaccination strategy that can potently accentuate effective ACT in non-lymphodepleted hosts.

Introduction

Adoptive cell transfer (ACT) with tumor-specific T cells is successfully applied in patients with post-transplant lymphoproliferative disease, leukemia, and melanoma [1-3]. Adoptively transferred T lymphocytes are frequently obtained from stem cell donors in the case of hematopoietic tumors, but also autologous T cells have the capacity to control the outgrowth of malignant cells. In melanoma, transfer of tumor-infiltrating lymphocytes that have been activated and expanded *in vitro* is capable of inducing the regression of large metastasized lesions and results in long-term survival in approximately half of the stage IV melanoma patients [3]. The function and maintenance of the transferred melanoma-reactive T cells were greatly improved when the recipients were pretreated with a lymphodepleting or even myeloablative regimen [3-6]. In the absence of host conditioning, the transferred T cells were hardly detectable after a few days, despite the fact that high doses of the T-cell growth factor interleukin (IL)-2 were provided. The "empty" host apparently promotes the proliferation and survival of the transferred T cells, leading to a more efficient tumor regression. Furthermore, lymphodepletion may help to overcome immune-suppressive mechanisms orchestrated by tumors [6-8]. These clinical findings on melanoma nicely illustrate that the patients' own T-cell repertoire does comprise functional tumor-specific lymphocytes, although their contribution to the natural tumor resistance seems to be limited. Therapeutic peptide vaccination aims at the recruitment of such endogenous tumor-specific T cells, but its clinical success has thus far been limited. Recently, we have observed much more robust immune and clinical responses following therapeutic vaccination when using longer peptides comprising T-cell epitopes [9,10]. The efficient activation of tumor-specific T cells that was observed in these patients did not depend on any kind of hematologic conditioning of the host, in contrast to the findings for ACT.

We here report on the combination treatment of ACT and peptide vaccination. Long peptides comprising the melanoma $gp100_{25-33}$ epitope were applied to activate adoptively transferred T cells *in vivo*. Extreme clonal expansions up to 1,000-fold and effective antimelanoma responses were observed in the absence of lymphodepletion. Our results imply that the field of T-cell–based immunotherapy reaches an era in which, next to clinical efficacy, also adverse immunopathology needs to be carefully evaluated.

8

Materials and Methods

Mice

C57BL/6jico mice, 8 weeks old, were obtained from Charles River (France). T-cell receptor (TCR) transgenic mice containing $gp100_{25-33}\backslash H\text{-}2D^b$ specific

receptors (designated as pmel; [11]) were a kind gift of Dr. N.P. Restifo (Center for Cancer Research, National Cancer Institute, NIH, Bethesda, MD) and were bred to express the congenic marker CD90.1 (Thy1.1). All animals were housed under specific pathogen-free conditions and cared for in accordance with the guidelines of the local University Committee for the Care of Laboratory animals (DEC), NIH guidelines on laboratory animal welfare, and the Association for Research in Vision and Ophthalmology statement for the Use of Animals in Ophthalmic and Vision Research.

Adoptive cell transfer and immunization of mice

Lymphocytes from the spleen and lymph nodes of naïve CD90.1-positive pmel mice were isolated and enriched for T lymphocytes by nylon wool. Enriched spleen cells (3×10^6 CD8$^+$ T lymphocytes) were adoptively transferred by injection into the tail vein. Mice were immunized 1 day later by shaving the left flank and s.c. injecting 150 μg of homologous human gp100$_{20-39}$ KVP (AVGAL<u>KVP</u>RNQDWLGVPRQL) or mouse gp100$_{20-39}$ EGS (AVGAL<u>EGS</u>RNQDWLGVPRQL) peptide solved in PBS. Toll-like receptor (TLR) ligands were simultaneously applied: 60 mg of Aldara cream containing 5% imiquimod on the skin at the injection site or 25 μg of CpG 1826 from the Leiden Institute of Chemistry. Immunizations were repeated on day 7 and then combined with two i.p. injections of 600,000 IU human recombinant IL-2 (Novartis) on the day of the second vaccination and one on the next day. To achieve slow release of gp100 peptide *in vivo*, 150-μg peptides were emulsified in Montanide-ISA-51 with PBS. Adoptive transfer of OT-1 cells and vaccination with long OVA peptide were described previously [12].

Melanoma treatment

The B16F10 melanoma cell line was derived from the American Type Culture Collection and fresh batches were thawed every year. No further authentication was used, but the expression of melanoma antigens and MHC-I molecules was tested during the experiments. Cells were cultured in Iscove's modified Dulbecco's medium (IMDM; Invitrogen) supplemented with 8% FCS (GIBCO), glutamine, and 2% penicillin/streptomycin. All cell lines were incubated at 37°C in a humidified atmosphere containing 5% CO_2. Subcutaneous melanomas were generated by s.c. injection of 2×10^4 B16F10 tumor cells in the flank. At day 5, when the melanoma was established, treatment with pmel T cells and peptide vaccination was started. Tumor size was measured twice a week with a caliper, and mice were sacrificed when tumors exceeded 1 cm^3 in size. Intraocular tumors were generated by inoculation of 4 μL containing 2.5×10^4 B16F10 cells in the anterior chamber under anesthesia, as previously described [13], using an injection needle derived from fused silica capillary (200-μm outer diameter, 100-μm inner diameter) fitted into a union (VALCO, Vici AG International). The capillary and the union were mounted onto a 0.1-mL Hamilton syringe. Tumor growth was measured three times a week with a dissecting microscope, and

mice were sacrificed when the eye was 80% to 100% occupied by tumor cells.

In vivo effector functions

Peripheral blood lymphocyte (PBL) samples were collected from tail veins and red blood cells were lysed for 10 minutes on ice. Cells were stained with the monoclonal antibodies anti-CD62L-phycoerythrin, anti-CD8-peridinin chlorophyll protein, and anti-90.1-allophycocyanin (BD Pharmingen); acquired on a Calibur flow cytometer (BD Biosciencess); and analyzed with CellQuest Pro software (BD Biosciencess). For determination of pmel T cells in the eyes and lymph nodes, mice were euthanized by cervical dislocation. After removal, eyes were incubated for 45 minutes at 37°C in a 5% CO_2 atmosphere in IMDM and 8% FCS supplemented with 250 units/mL collagenase IV (Sigma-Aldrich) and 50 µg/mL DNase (Sigma-Aldrich). Eyes were then pressed over a cell strainer to generate single-cell suspensions. Lymph nodes and spleen were directly pressed through a cell strainer. For intracellular cytokine staining of IFN-γ, PBL were incubated overnight with mouse gp100 peptide EGSRNQDWL (1 µg/mL) stimulation at 37°C in a 5% CO_2 atmosphere and stained as described before [14]. The capacity of ACT-treated and immunized mice to eradicate peptide-pulsed target cells was analyzed as previously described [14].

Histology and immunohistochemistry

Enucleated eyes and organs were embedded in Tissue-Tek optimum cutting temperature (Sakura Fine-Tek) for cryosections or fixed in 4% buffered neutralized formalin for paraffin sections. Four-micrometer-thick serial sections were mounted on a slide; routine staining was performed with H&E on paraffin sections. Staining with anti-CD90.1 was performed on cryosections with a 1:1,000 dilution of biotin-labeled mouse anti-mouse antibody (clone HIS51, eBioscience). Paraffin sections were stained for CD3 with a polyclonal rabbit anti-human/mouse CD3 diluted 1:800 (clone A0452, Dako). Subsequently, biotinylated swine anti-rabbit IgG antibody (clone E0431, Dako) was used at 1:100 as secondary antibody. Stainings were visualized with alkaline phosphatase-streptavidin, diluted 1:100 (clone no. K0391, Dako), and developed with Fast Red (Scytek) in naphthol-phosphate buffer (Scytek) with 50 mmol/L levamisole. The slides were counterstained with Mayer's hematoxylin. Control sections were incubated with secondary antibodies alone.

Cytokine and blood chemistry analysis

A cytometric bead array (BD Biosciences) was performed on inflammatory cytokines [IL-12p70, IL-6, IL-10, tumor necrosis factor-α (TNF-α), IFN-γ, and MCP-1] in serum obtained by heart puncture. Blood samples were centrifuged at 10,000 rpm for 10 minutes and were diluted 1:4 for CBA analysis, according to the manufacturer's instruction, and analyzed on a Calibur machine with CellQuest software (BD). Standard curves were included for each cytokine

8

to determine blood concentrations. Samples of 150 μL of heparin blood from cardiac punctures were analyzed for functions of renal (creatinine) and liver aspartate aminotransferase (AST), alanine aminotransferase (ALT), and total bilirubin with a fully automated Modular P 800 system (Roche). All coefficient variations were below 3%.

Statistical analysis

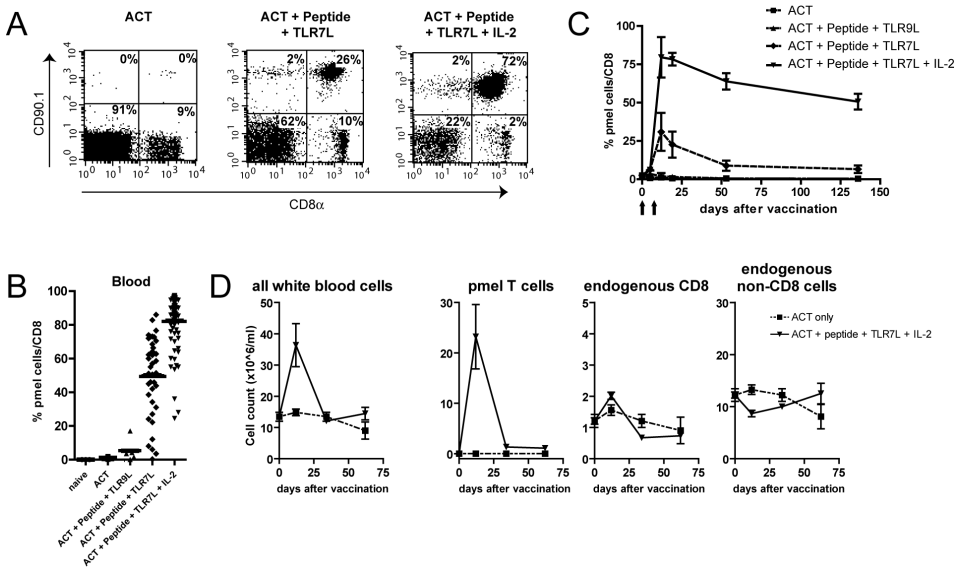Statistical analyses were performed using GraphPad software. The precise statistical method that was applied is indicated in the figure legends.

Figure 1. Massive clonal expansion and persistence of pmel T cells after peptide vaccination. **(A)** representative flow cytometry plots of peripheral blood of mice receiving T-cell receptor transgenic pmel T cells with or without vaccination with 20-mer long peptide comprising the cognate gp100 peptide epitope. After ACT of pmel T cells (ACT), mice were vaccinated twice with gp100 peptide in PBS (peptide), topical imiquimod adjuvant (TLR7L), and low-dose IL-2 (IL-2). CD90.1 is selectively expressed on the adoptively transferred cells. Samples were taken on day 12, 5 d after the last peptide vaccine. **(B)** frequencies of pmel T cells as part of all CD8$^+$ cells in peripheral blood are shown with their means (lines) per group. Imiquimod (TLR7L) or CpG oligonucleotide (TLR9L) was used as adjuvant. Each dot represents one mouse. Samples were taken 5 d after the last peptide vaccine. **(C)** frequencies of pmel T cells were measured over time from blood lymphocytes. Arrows indicate vaccinations (day 0 and day 7). Points, mean of three mice per group from one of four experiments with comparable outcome; bars, SD. **(D)** white blood cell counts in blood were calculated by measuring the absolute number of blood cells and determining the frequencies by flow cytometry. Separate populations were determined on the basis of CD90.1 and CD8 staining: pmel T cells (CD90.1$^+$CD8$^+$), endogenous CD8 cells (CD90.1$^-$CD8$^+$), and endogenous non-CD8 cells (CD90.1$^-$CD8$^-$). Points, mean of four mice; bars, SD.

Results and Discussion

In vivo T-cell activation by long peptide causes massive T-cell expansion and persistence

Immunization with a 20-amino-acid long peptide comprising the human version of the gp100$_{25-33}$ CTL epitope activated melanocyte-specific T cells from the endogenous T-cell repertoire but failed to control the outgrowth of B16 melanomas [14]. We then analyzed the effects of peptide vaccination after adoptive transfer of gp100$_{25-33}$–specific TCR-transgenic pmel T cells. Strong expansions of T cells were observed after s.c. immunization with peptide in PBS and topically applied imiquimod, a TLR7 ligand (TLR7L; Fig. 1A). Five days after the second immunization, around 50% of all CD8$^+$ T cells in the blood were pmel cells, as determined with the CD90.1 congenic marker on the transferred pmel T cells. Addition of low-dose IL-2 even enhanced this frequency up to 90% (Fig. 1A and B), showing that the CD8$^+$ T-cell pool was heavily skewed toward the transferred T cells. Comparable high frequencies were observed in the spleen and lymph nodes, indicating that the *in vivo* activated pmel T cells spread systemically (Supplementary Fig. S1). Peptide and imiquimod were both essential for the massive clonal expansions of pmel T cells *in vivo* (Supplementary Fig. S2A), as replacement of imiquimod with TLR9L CpG DNA resulted in much lower frequencies (Fig. 1B).

Measurement of the pmel T-cell frequencies over time revealed a strong increase of pmel T-cell frequencies up to the week after the last immunization and then a slow contraction of this population (Fig. 1C). Notably, even 120 days after the last immunization, the peripheral CD8$^+$ T-cell compartment of mice treated with ACT, peptide, imiquimod, and IL-2 still consisted of more than 50% pmel cells, pointing at a very high abundance of memory T cells. These memory T cells produced IFN-γ on brief *in vitro* stimulation (Supplementary Fig. S2B) and stained positive for the lymph node–homing molecules CD62L and CD27 (Supplementary Fig. S2C), showing a normal memory phenotype and function [15]. Similar dynamics were found with 10 times less transferred T cells (Supplementary Fig. S2A) or in the context of the independent OT-1 TCR-transgenic T cells and OVA peptide model (Supplementary Fig. S2D), indicating that these striking expansions and high memory frequencies were commonly found in ACT combined with this vaccine consisting of long peptide, imiquimod, and IL-2.

Phenotypic analysis of the blood of these mice seemed to suggest that the numbers of endogenous hematopoietic cells of other lineages were strongly decreased after vaccination (CD90.1$^-$CD8$^-$ cells in Fig. 1A). However, this was only a relative decrease because the total white blood cell count tripled owing to the extreme pmel T-cell expansions (Fig. 1D). The absolute numbers of the

8

endogenous hematopoietic cells, including red blood cell counts, were hardly affected (Fig. 1D). Our data implied that peptide vaccination with imiquimod and IL-2 induces a 1,000-fold expansion of adoptively transferred T cells. Previous findings with this model also showed that transferred pmel T cells need *in vivo* activation or otherwise remain ignorant to the endogenous gp100-expressing melanocytes. However, immunization with antigen-encoding DNA, short peptides, or recombinant viruses, as previously tested, did not yield the extreme expansions that we observed here [4,11,16-19]. Apparently, the combination of peptide in PBS, a topical overlay of imiquimod, and a low dose of IL-2 is optimally stimulating to CD8+ T cells. The same dynamics were observed in the OVA-specific OT-1 model, indicating that the effect of this vaccine mixture is not limited to the pmel system. The importance of imiquimod is further underlined by the finding that replacement with TLR9L CpG resulted in much less T-cell expansions. It is known that topically applied imiquimod leads to strong skin infiltration of dendritic cells [4,20]. We would like to emphasize that these striking CD8+ T-cell dynamics were obtained in immunocompetent hosts in the absence of lymphodepletion or other hematologic conditioning.

In vivo effector functions of transferred T cells

The heavily expanded pmel T cells were examined for effector functions *in vivo*. First, fluorescence-labeled and peptide-loaded spleen cells were injected as target cells. These targets were efficiently killed in vaccinated mice that received pmel T cells, whereas target cells loaded with a control peptide were still detectable (Supplementary Fig. S3A and B). Interestingly, the low pmel frequencies in the TLR9L group were sufficient to eliminate all gp100-loaded targets, pointing at the sensitivity of this assay. Second, we scored the degree of skin depigmentation, which is a result of on-target pathology due to elimination of gp100-positive skin-residing melanocytes. All animals receiving pmel T cells and peptide vaccination showed depigmentation after 2 to 3 months, indicating that the activated T cells were capable of skin infiltration and eradication of healthy gp100-expressing melanocytes (Supplementary Fig. S3C and D). Depigmentation was most obvious at the site of imiquimod application on the flank, but in mice receiving additional low-dose IL-2 injections, the whiskers and eyelids turned white as well. Interestingly, intentional skin injury in these mice by a short tattoo treatment resulted in focused white spots in the fur at the site of tattooing (data not shown), suggesting that local on-target damage to healthy skin melanocytes depends on tissue responses evoked by imiquimod- or tattooing-mediated inflammatory signals.

Third, we tested the capacity of pmel T cells to eradicate subcutaneous B16 melanomas. Treatment of established melanomas was successful in half of the mice and tumor growth was delayed in the other mice (Fig. 2A). Finally, to challenge the tumor-protective capacity of our treatment modality, we investigated the tumor growth of melanomas in the anterior chamber of the eye. The eye is defined as an immune-privileged site harboring distinct
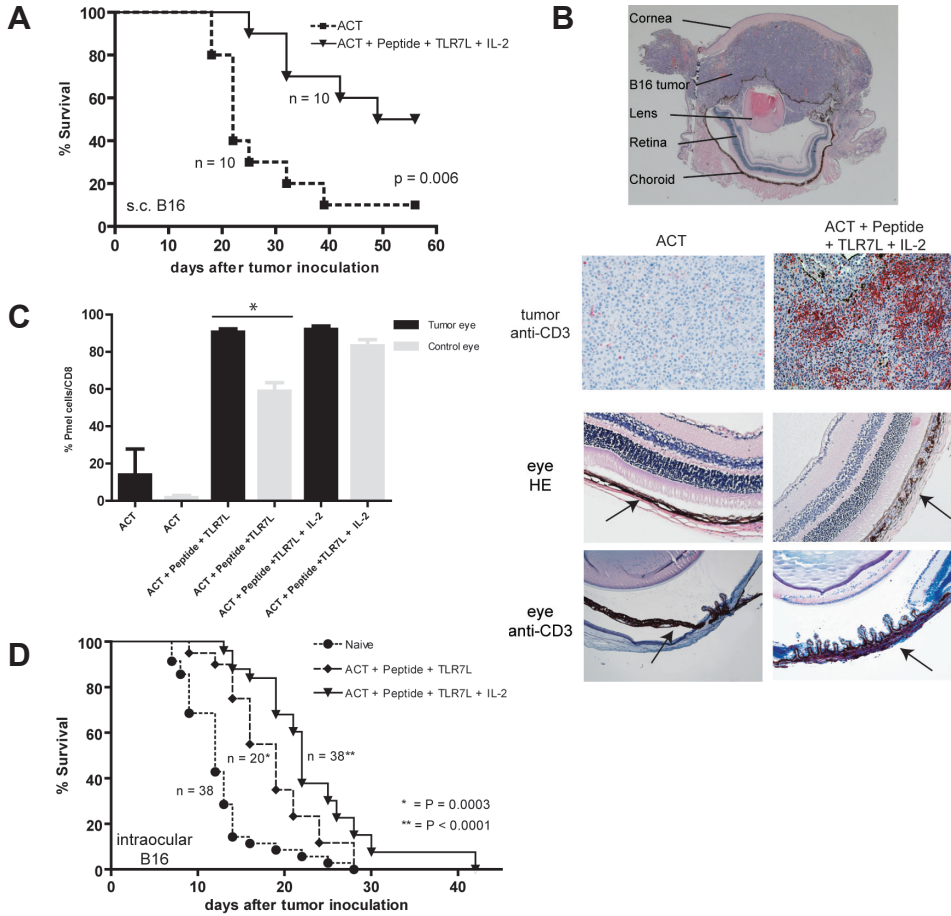
Figure 2. Effective homing and melanoma control by combination treatment. **(A)** mice were injected s.c. with B16F10 melanoma cells and treated with ACT alone or in combination with peptide, TLR7L, and IL-2 at day 5. The survival curves of these two groups are significantly different (log-rank test). Mice were sacrificed when tumor volume exceeded 1 cm³. Tumor growth in naïve mice was comparable to that of mice receiving only ACT (data not shown). Comparable results were found in an independent experiment. **(B)** H&E staining of an enucleated eye with an established B16F10 melanoma in the anterior chamber (top). Eyes were paraffin-embedded and stained for H&E or CD3 after ACT of pmel T cells and peptide vaccination. Arrows point to the gp100-positive uvea structure that is significantly thickened due to massive infiltration of pmel T cells (bottom). Cryosections with anti-CD90.1 staining gave similar patterns (not shown). **(C)** bar graphs of pmel T-cell infiltration in the tumor-bearing eyes and control eyes. Treatment with ACT alone did not result in homing to the eyes, but addition of peptide vaccination showed a strong infiltration of pmel T cells. Hardly any endogenous T cells infiltrated the eye. Indicated percentages represent frequencies of pmel T cells of total CD8⁺ cells. Frequencies of pmel T cells in control eyes were lower than those in tumor eyes in the group without IL-2 (*, P = 0.001, Student's t test). Columns, mean of five animals per group from one of three independent experiments; bars, SD. **(D)** a delay in intraocular B16F10 melanoma outgrowth was observed in mice treated with ACT and peptide vaccination. Both treatment groups were significantly different from the control group (log-rank test). Figure shows compiled data from three independent experiments that all displayed significant differences between the groups.

8

immunosuppressive mechanisms [21]. We inoculated B16 melanoma cells in the anterior chamber of the eye using microinjections, reflecting uveal melanoma in humans. Progressive and fast melanoma outgrowth was observed, and mice were sacrificed when the tumor completely filled this site, which was already achieved in most mice after 2 weeks (Fig. 2B). *In vivo* activated pmel T cells homed to both eyes regardless of the presence of B16 melanoma (Fig. 2C). Interestingly, homing to the eyes was scarcely accompanied with entry of other $CD8^+$ T cells, and animals receiving only transferred pmel cells hardly contained $CD8^+$ T cells at all (Fig. 2C). Addition of low-dose IL-2 to the protocol resulted in the highest level of pmel T-cell infiltrate. We stained tissue sections of the B16 tumors with CD3- and CD90.1-specific antibodies and confirmed that the pmel T cells were located within the tumor beds in close contact with tumor cells (Fig. 2B and data not shown). Furthermore, large numbers of T cells were found in the gp100-expressing choroidal layer of the uvea, even in control eyes (Fig. 2B). This structure of the eye was clearly thickened compared with the mice receiving pmel T cells alone. These findings are similar to recently published data on uveitis in a mouse model and a cutaneous melanoma patient who was treated with immunotherapy [22,23]. Importantly, treatment with ACT and peptide vaccination caused a significant delay in B16 melanoma outgrowth in the eye compared with naïve mice (Fig. 2D). This delay was even more pronounced when low-dose IL-2 was added to the treatment regimen. The limited treatment efficacy might be due to the immunosuppressive environment of the anterior chamber of the eye. In conclusion, *in vivo* activation of adoptively transferred T cells by peptide vaccination endows these T cells with the capacity to home to the skin and eyes and mediate tumor control at these sites.

Lethal cytokine storm after continued peptide vaccination

When mice were vaccinated with long peptide and imiquimod for a third time, they presented with fever chills, ataxia, and ruffled fur. These symptoms were apparent after 5 hours and resulted in death in 25% of the animals within 12 hours. Addition of low-dose IL-2 increased the percentage of death to 90% (Table 1). We observed that pmel T-cell frequencies in the blood were correlated to these side effects, as mice with more than 85% pmel T cells before the third vaccination all succumbed to the peptide vaccination protocol, whereas mice with lower pmel frequencies showed symptoms but did not die (Table 1). The pathophysiologic cause underlying these unexpected side effects was investigated by blood analyses and autopsies. Blood chemistry of sera taken from the mice at 10 hours after the last vaccination revealed strongly elevated levels of the liver enzymes AST, ALT, and creatinine, indicating liver and kidney damage (Supplementary Fig. S4A), whereas total bilirubin was not different between the treatment and control groups (data not shown). Again, the addition of low-dose IL-2 led to more pronounced toxicity. H&E staining of lungs, spleens, livers, and kidneys of mice before and after the last peptide vaccination showed tremendous differences in tissue structure (Fig. 3A). The splenic architecture was disrupted, as no clear white pulp zones were visible anymore. The lungs were massively infiltrated with neutrophil

granulocytes and T cells, and also the livers and kidneys showed clear signs of immunopathology (Fig. 3A). Together, these data suggested multiorgan failure as cause of death.

Table 1. Symptoms of systemic inflammatory response syndrome after treatment

Treatment modality	Adverse effects			pmel frequencies[c]
	Number of mice ill[a]	Symptom severity	Number of mice dead[b]	
naive	0/10 (0%)	-	0/10 (0%)	0.0
ACT	0/10 (0%)	-	0/10 (0%)	0.8
ACT + peptide + TLR7L	20/20 (100%)	+	5/20 (25%)	57.0
ACT + peptide + TLR7L + IL-2	20/20 (100%)	+++	18/20 (90%)	88.0

[a] Symptoms were fever chills, ataxia and gathering.
[b] After 24 hours of last vaccination.
[c] Means of pmel frequency of CD8+ T cells in peripheral blood.

Blood samples at 5 and 10 hours after the third vaccination were also analyzed for six different cytokines: IL-12, IFN-γ, IL-10, MCP-1, TNF-α, and IL-6 (Fig. 3B). The proinflammatory cytokine IL-12 was not elevated in the diseased animals, whereas all the other cytokines were strikingly high. In line with the degree of mortality, vaccination without IL-2 resulted in a peak at 5 hours and a subsequent decrease. Most of these mice spontaneously recovered from cytokine storm symptoms. However, cytokine levels remained high in the group with inclusion of IL-2. Of note, these extreme cytokine levels were not found after two vaccinations with peptide and strictly correlated with clinical symptoms (Table 1). We reasoned that the multiorgan failure was caused by cytokine storm and resembled an aseptic systemic inflammatory response syndrome (SIRS), an immune-mediated constitution found in severe graft-versus-host disease; antithymocyte globulin injection for prevention of transplant rejection; and acute respiratory distress syndrome, in which the lungs are injured intrinsically or by trauma [24-26]. However, the closest resemblance is found in the recently published clinical studies of agonistic anti-CD40 and anti-CD28 administration [27,28]. This latter study, which was conducted in healthy young volunteers, was not successful because massive cytokine release by T cells was accompanied with serious multiorgan failure; fortunately, the lives of all subjects were saved with the use of corticosteroids and *in vivo* capture of IL-2 [27].

Prevention of SIRS with peptides in a slow-release depot or weak agonistic peptides

Long peptides were administered in a physiologic salt solution in this study because this formulation is known to mediate excellent *in vivo* T-cell priming when a strong adjuvant is provided [10,12]. The observed fast and massive cytokine release by pmel T cells after the third vaccination (Fig. 3) suggested that the

8

20-mer long peptides used in the current study quickly diffused from the s.c. injection site and thereby systemically stimulated pmel T cells. Our previous studies on long peptides, however, indicated that long peptides are only drained to the local lymph node [10,12]. Indeed, the biodistribution of the 20-mer long gp100 peptide was largely restricted to the local draining lymph node, in contrast to the minimal 9-mer peptide epitope, which was also detected at the distant contralateral side (Fig. 4A). Higher quantities of the long peptide resulted in systemic spread. We concluded that a local pulse of peptide presentation was sufficient for fast and vigorous stimulation of pmel T cells leading to fatal cytokine storm and multiorgan failure.
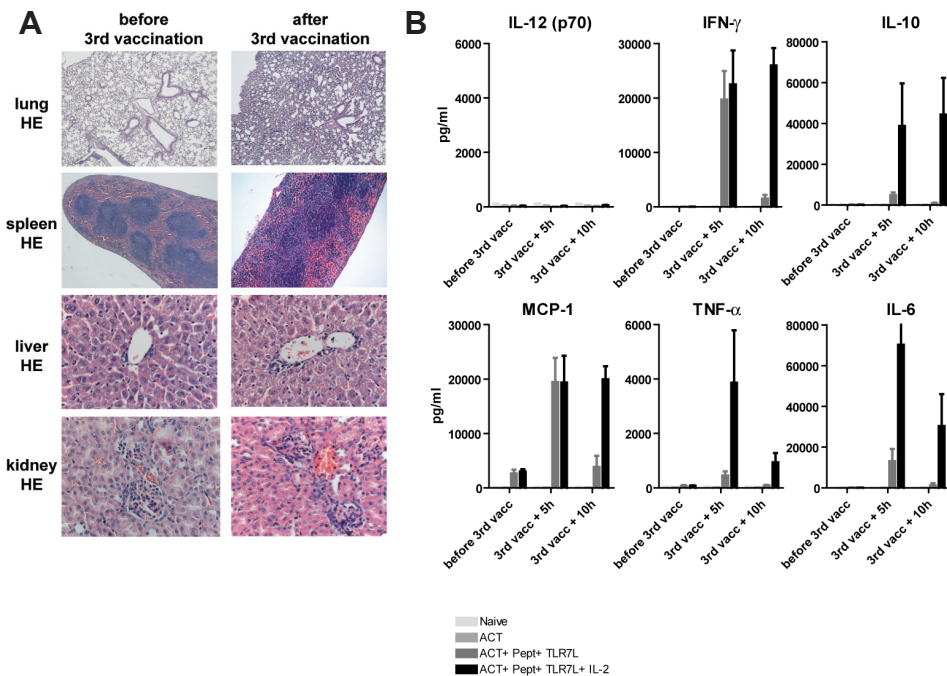
Figure 3. A third vaccination with peptide results in multiorgan failure and cytokine storm. Mice treated with ACT of pmel T cells and vaccination with gp100 peptide, TLR7L, and low-dose IL-2 presented with fever chills and ataxia and died within 24 h. **(A)** histologic analysis of the lung, spleen, liver, and kidney showing immunopathology. Tissues were taken just before (left) and 10 h after (right) the third vaccination. A summary of toxicity is shown in Table 1. **(B)** the serum levels of cytokines in animals from different treatment groups were determined. Columns represent different treatment groups: naïve mice (light gray); ACT of pmel only (medium gray); ACT, peptide vaccination, and TLR7L (dark gray); and treatment including IL-2 (black). Sera were taken on different time points: before, 5 h after, and 10 h after the third vaccination. Each group contained five mice. Columns, mean; bars, SD. Comparable data were obtained in an independent experiment.
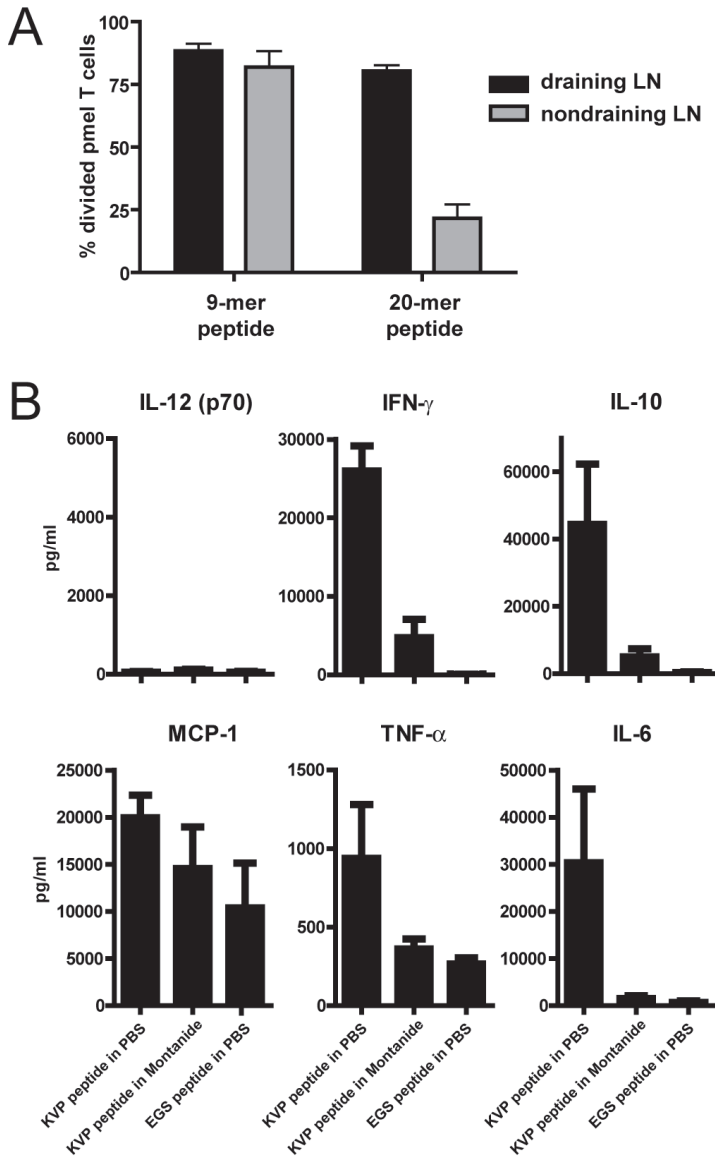
Figure 4. Prevention of peptide spread and cytokine storm by mineral oil formulation or weak agonistic peptides. **(A)** s.c. injection of gp100 peptide in PBS gave a pulse of peptide spread in the local injection area. Naïve mice were injected with equimolar amounts of 9-mer or 20-mer gp100 peptide together with TLR7L. Local draining lymph nodes and distant contralateral mesenteric lymph nodes were removed after 1 d, dispersed, and used as presenting cells for carboxyfluorescein diacetate succinimidyl ester–labeled pmel T cells in vitro. MHC class I presentation was expressed as percentage of pmel T cells that divided. The 9-mer peptide clearly reached the distant lymph node, whereas the 20-mer peptide only resided in the local lymph node. Columns, mean of five mice per group from one of three independent experiments; bars, SD. **(B)** mice were treated with ACT of pmel T cells and vaccination with 20-mer long gp100-peptide comprising the strongly binding CTL epitope (KVP) in PBS, the same peptide emulsified in mineral oil Montanide, or a long peptide comprising the weak agonist CTL epitope (EGS) in PBS. Serum cytokines were measured 10 h after the third vaccination. Each group contained 10 mice. Columns, mean; bars, SD.

To prevent cytokine storm, we replaced the PBS in the third vaccination with the mineral oil Montanide-ISA-51 to restrain the release of the peptide. This completely prevented the symptoms of SIRS, despite high pmel T-cell frequencies. The levels of liver enzymes and creatinine and the concentrations of cytokines confirmed the absence of morbidity and massive pmel T-cell activation (Supplementary Fig. S4B; Fig. 4B). Alternatively, vaccination with a long peptide comprising the wild-type sequence of mouse gp100 (EGSRNQDWL) also prevented SIRS (Fig. 4B). This peptide epitope binds with less affinity to the presenting MHC class I molecule and is a weaker agonist than the widely used altered peptide (KVPRNQDWL; [14]). These results showed that the strong immunopathology of SIRS could be prevented either by applying weak agonistic peptides or by formulating the peptide in a slow-release depot, such as mineral oil. Thus, the adverse effect of the massive T-cell activation by peptide vaccination can be readily prevented.

In clinical studies of adoptive cell therapy, hematologic conditioning has been considered necessary for optimal T-cell activation and antitumor efficacy [5,7,29,30]. The mechanisms involved are likely quite diverse: creating physical space for the introduced cells, removal of cytokine "sinks" and suppressor cells, and activation of antigen-presenting cells through the intestinal flora [7]. Here, we show that a 1,000-fold expansion of T cells and antitumor efficacy can also be observed in immunocompetent, nonconditioned hosts. This sheds new light on the previously defined requirements and might open up possibilities of reaching clinical tumor responses without severe pretreatment conditioning of the patient. The combination of ACT with peptide vaccine–mediated activation *in vivo* and TLR ligands, as applied in our study, is certainly an avenue for further exploitation in cancer therapy. However, the power of this combination also warrants precautions concerning overstimulation of tumor-specific CD8+ T cells when the levels of circulating specific T cells are pushed to the limit. Harnessing this power is imperative and must include careful peptide formulations that prevent rapid spread of the peptide, for example, by using slow-release adjuvant or optimal peptide design.
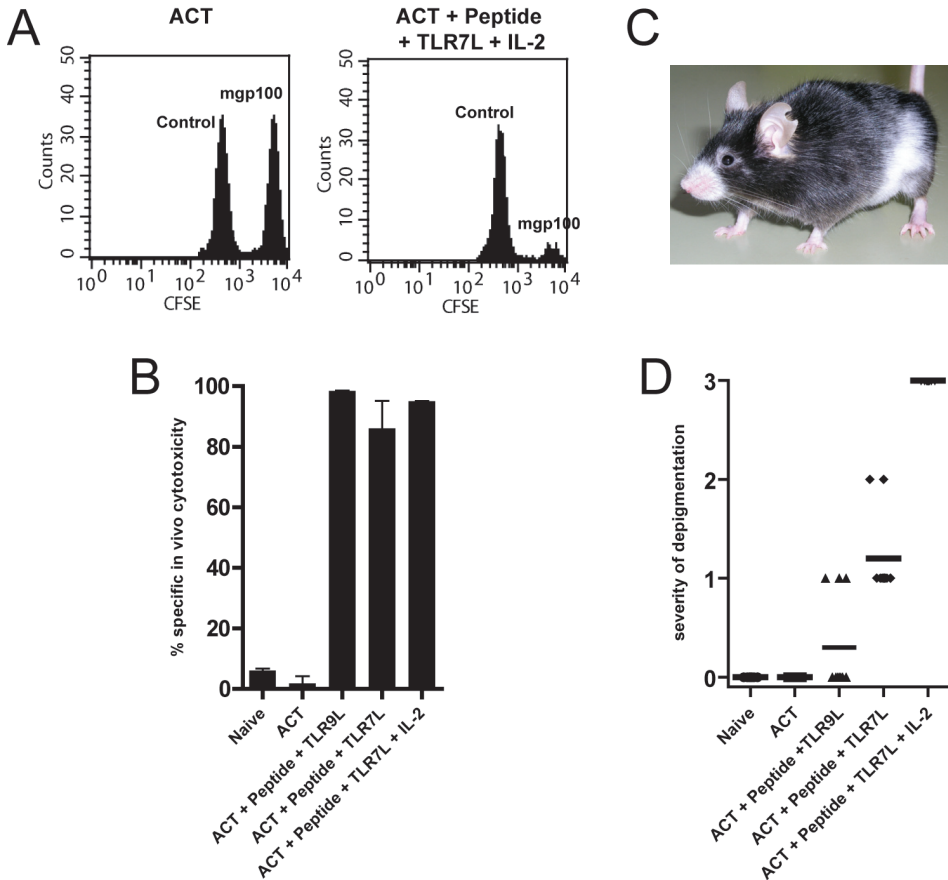
Supplementary data
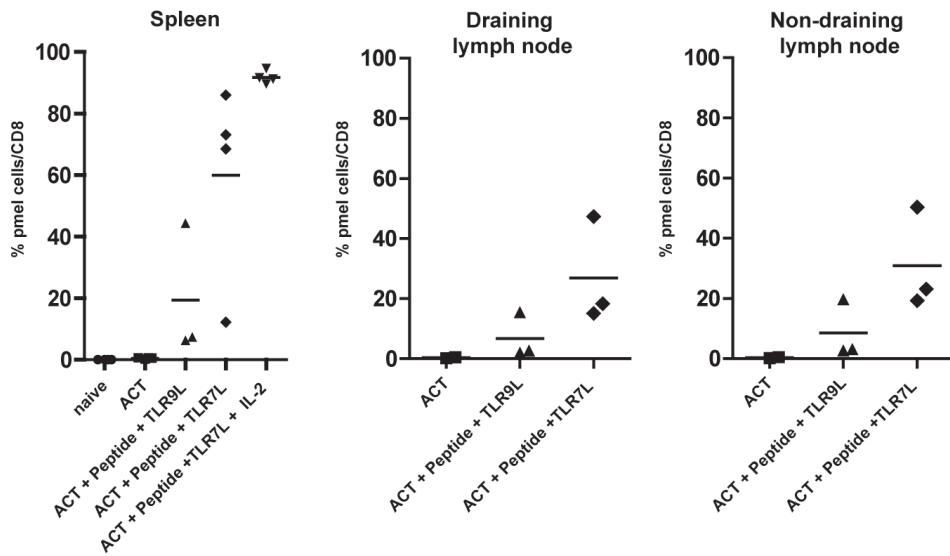
Supplementary figure S1. Presence of pmel T cells in spleen and lymph nodes.
Percentage of pmel T cells in the spleen, draining and non-draining lymph nodes in mice undergoing different treatment protocols. Samples were all taken 12 days after the first vaccination, when two treatment sessions had taken place. Adoptive cell therapy ('ACT') in combination with 20-mer long gp100 peptide ('peptide'), topical application of imiquimod ('TLR7L') and low dose IL-2 resulted in the highest frequencies of pmel T cells in lymph nodes.

8
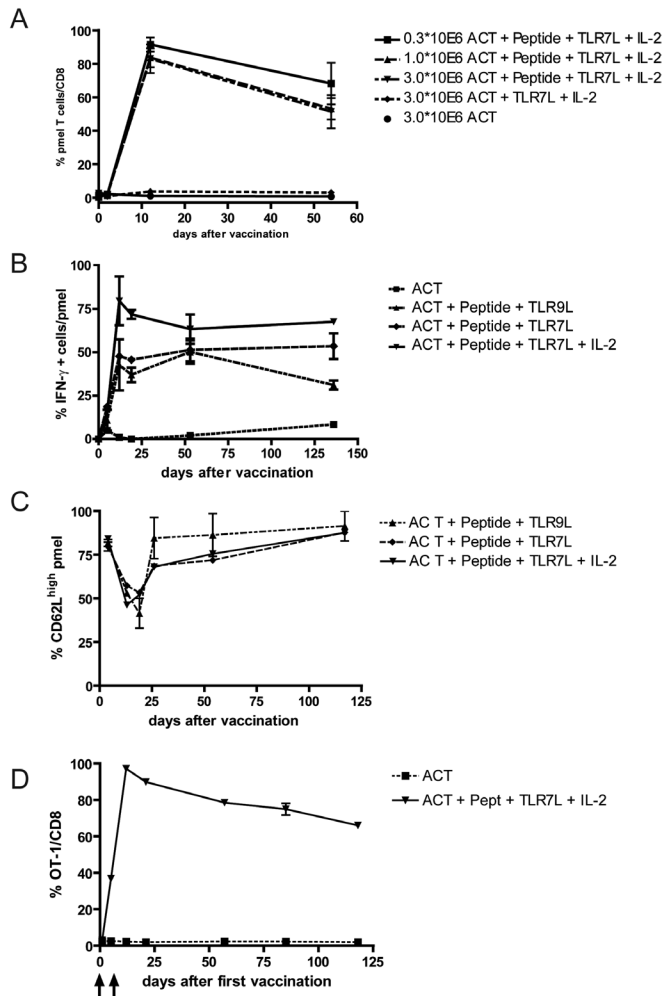
Supplementary figure S2. Massive clonal expansion induced by peptide vaccination.
(A) Different numbers of pmel T cells ('ACT') were injected i.v. and recipient mice were vaccinated with 20-mer long peptide, TLR7L and IL-2. As controls, mice were treated without peptide or treated with ACT only. Mice were vaccinated twice with peptides at day 0 and day 7. Blood frequencies of pmel T cells out of the total pool of $CD8^+$ cells were determined by flow cytometry. Transfer with ten times less T cells provided similar frequencies in the blood during the expansion and contraction phase. Data represent means and standard deviations of five mice per group **(B)** IFN-γ release by pmel cells measured after a brief overnight stimulation with the natural mouse gp100 peptide. Percentage of IFN-γ producing pmel out of all pmel T cells is shown. Means and standard deviations of three mice per data group are shown from one out of four experiments with comparable outcome. **(C)** Expression of CD62L was measured on adoptively transferred pmel T cells. The percentage CD62L^{high} cells out of the total pmel T cells pool in the blood was determined by flow cytometry using staining with CD90.1, CD8 and CD62L. Re-expression of CD62L and CD27 (not shown) from day 35 indicates that the expanded pmel T cells developed into central memory T cells. **(D)** Ovalbumine-specific transgenic T cells (OT-I) were transferred into naïve mice and activated with vaccine consisting of long OVA peptide, TLR-7L and IL-2. The frequencies of OT-I cells as part of all $CD8^+$ T cells in peripheral blood were measured over time from blood lymphocytes. Arrows indicate the time of peptide vaccination (day 0 and 7). Mean and standard deviation of three mice per group is shown.

Supplementary figure S3. In vivo function of expanded pmel T cells.
(A) Mice treated with adoptive cell transfer of pmel T cells and vaccination with 20-mer long peptide lysed peptide-loaded target cells in vivo. Target cells from naïve spleens were in vitro loaded with short mouse gp100 peptide and high dose of CFSE or control Db-binding peptide and low dose CFSE and injected into immunotherapy treated animals. After two days the spleens of the recipient animals were harvested and analyzed for percentage of specific killing of gp100-peptide loaded targets. **(B)** Overview of the in vivo killing assay as described above. Treatment modalities are depicted on the X-axis. Each treatment group contained five mice and means and standard deviations are shown from one out of three comparable results. **(C)** The depigmentation status of a mouse that was treated with adoptive cell transfer, gp100 peptide, TLR7L and low dose IL-2 after six months. The white fur at the flank indicates the application site of TLR7L, which was topically applied in a cream on the skin at the peptide injection site. The whiskers and eyelids also turned white, as well as scattered spots in the fur. **(D)** After six months, the degree of depigmentation was scored in all groups, where 0= no depigmentation, 1= signs of local depigmentation at the peptide injection site, 2= strong depigmentation at the injection site, 3= depigmentation of whiskers, eyelids and scattered depigmentation on the fur. Each dot represents one mouse (n=8 per group).

8
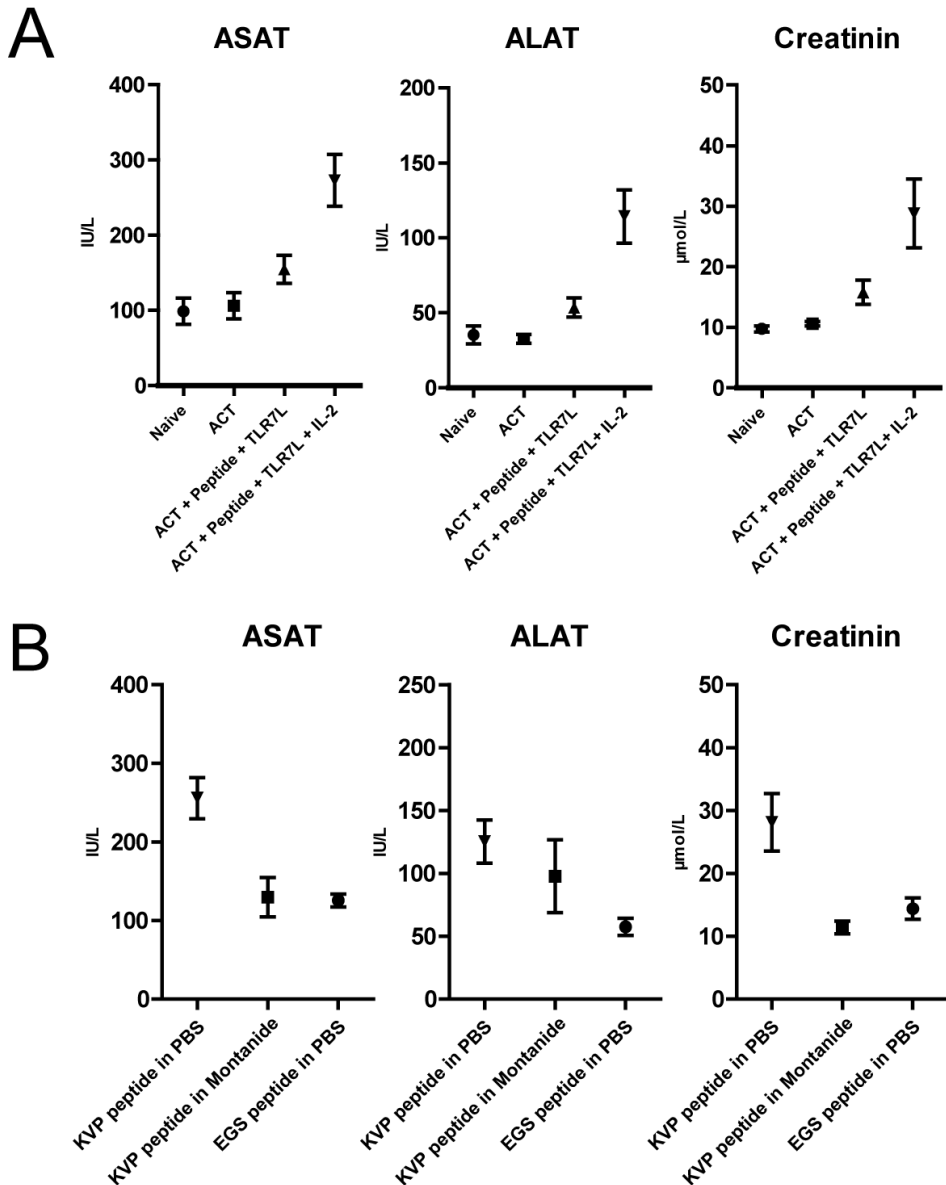
Supplementary figure S4. Blood chemistry of mice undergoing SIRS symptoms and mice treated with mineral oil or weak agonistic peptides to prevent SIRS.

Blood chemistry on liver enzymes (ASAT, ALAT) and renal function (Creatinin) are shown from blood samples 10 h after the third vaccination. **(A)** Mice were vaccinated with long peptide dissolved in PBS, resulting in SIRS syndrome with an apparent multi-organ failure, which is reflected by the blood chemistry. **(B)** Mice treated with the strong agonistic peptide dissolved PBS (as in A), or in mineral oil Montanide or with weakly agonistic EGS peptide in PBS. Means and standard deviations of five mice are shown.

Disclosure of Potential Conflicts of Interest

Acknowledgments

Grant Support

8

References

1.	Brentjens, R. J. *Cellular therapies in acute lymphoblastic leukemia.* Curr.Opin.Mol.Ther. 2009. 11:375-382.

2.	Leen, A. M., Rooney, C. M., and Foster, A. E. *Improving T cell therapy for cancer.* Annu.Rev. Immunol. 2007. 25:243-265.

3.	Rosenberg, S. A., Restifo, N. P., Yang, J. C., Morgan, R. A., and Dudley, M. E. *Adoptive cell transfer: a clinical path to effective cancer immunotherapy.* Nat.Rev.Cancer 2008. 8:299-308.

4.	Kohlmeyer, J., Cron, M., Landsberg, J., Bald, T., Renn, M., Mikus, S., Bondong, S., Wikasari, D., Gaffal, E., Hartmann, G., and Tuting, T. *Complete regression of advanced primary and metastatic mouse melanomas following combination chemoimmunotherapy.* Cancer Res. 2009. 69:6265-6274.

5.	Wrzesinski, C. and Restifo, N. P. *Less is more: lymphodepletion followed by hematopoietic stem cell transplant augments adoptive T-cell-based anti-tumor immunotherapy.* Curr.Opin.Immunol. 2005. 17:195-201.

6.	Zhou, Q., Bucher, C., Munger, M. E., Highfill, S. L., Tolar, J., Munn, D. H., Levine, B. L., Riddle, M., June, C. H., Vallera, D. A., Weigel, B. J., and Blazar, B. R. *Depletion of endogenous tumor-associated regulatory T cells improves the efficacy of adoptive cytotoxic T-cell immunotherapy in murine acute myeloid leukemia.* Blood 2009. 114:3793-3802.

7.	Klebanoff, C. A., Khong, H. T., Antony, P. A., Palmer, D. C., and Restifo, N. P. *Sinks, suppressors and antigen presenters: how lymphodepletion enhances T cell-mediated tumor immunotherapy.* Trends Immunol. 2005. 26:111-117.

8.	Overwijk, W. W. *Breaking tolerance in cancer immunotherapy: time to ACT.* Curr.Opin.Immunol. 2005. 17:187-194.

9.	Kenter, G. G., Welters, M. J., Valentijn, A. R., Lowik, M. J., Berends-van der Meer DM, Vloon, A. P., Essahsah, F., Fathers, L. M., Offringa, R., Drijfhout, J. W., Wafelman, A. R., Oostendorp, J., Fleuren, G. J., van der Burg, S. H., and Melief, C. J. *Vaccination against HPV-16 oncoproteins for vulvar intraepithelial neoplasia.* N.Engl.J Med. 2009. 361:1838-1847.

10.	Melief, C. J. and van der Burg, S. H. *Immunotherapy of established (pre)malignant disease by synthetic long peptide vaccines.* Nat.Rev.Cancer 2008. 8:351-360.

11.	Overwijk, W. W., Theoret, M. R., Finkelstein, S. E., Surman, D. R., de Jong, L. A., Vyth-Dreese, F. A., Dellemijn, T. A., Antony, P. A., Spiess, P. J., Palmer, D. C., Heimann, D. M., Klebanoff, C. A., Yu, Z., Hwang, L. N., Feigenbaum, L., Kruisbeek, A. M., Rosenberg, S. A., and Restifo, N. P. *Tumor regression and autoimmunity after reversal of a functionally tolerant state of self-reactive CD8+ T cells.* J Exp.Med. 2003. 198:569-580.

12.	Bijker, M. S., van den Eeden, S. J., Franken, K. L., Melief, C. J., van der Burg, S. H., and Offringa, R. *Superior induction of anti-tumor CTL immunity by extended peptide vaccines involves prolonged, DC-focused antigen presentation.* Eur.J Immunol. 2008. 38:1033-1042.

13.	Schurmans, L. R., den Boer, A. T., Diehl, L., van der Voort, E. I., Kast, W. M., Melief, C. J., Toes, R. E., and Jager, M. J. *Successful immunotherapy of an intraocular tumor in mice.* Cancer Res. 1999. 59:5250-5254.

14.	van Stipdonk, M. J., Badia-Martinez, D., Sluijter, M., Offringa, R., van Hall, T., and Achour, A. *Design of agonistic altered peptides for the robust induction of CTL directed towards H-2Db in complex with the melanoma-associated epitope gp100.* Cancer Res. 2009. 69:7784-7792.

15.	Northrop, J. K. and Shen, H. *CD8+ T-cell memory: only the good ones last.* Curr.Opin.Immunol. 2004. 16:451-455.

16.	Hosoi, A., Takeda, Y., Furuichi, Y., Kurachi, M., Kimura, K., Maekawa, R., Takatsu, K., and Kakimi, K. *Memory Th1 cells augment tumor-specific CTL following transcutaneous peptide immunization.* Cancer Res. 2008. 68:3941-3949.

17.	Saenger, Y. M., Li, Y., Chiou, K. C., Chan, B., Rizzuto, G., Terzulli, S. L., Merghoub, T., Houghton, A. N., and Wolchok, J. D. *Improved tumor immunity using anti-tyrosinase related protein-1 monoclonal antibody combined with DNA vaccines in murine melanoma.* Cancer Res. 2008. 68:9884-9891.

18.	Salem, M. L., Diaz-Montero, C. M., Al Khami, A. A., El Naggar, S. A., Naga, O., Montero, A. J., Khafagy, A., and Cole, D. J. *Recovery from cyclophosphamide-induced lymphopenia results in expansion of immature dendritic cells which can mediate enhanced prime-boost vaccination antitumor responses in vivo when stimulated with the TLR3 agonist poly(I:C).* J Immunol. 2009. 182:2030-2040.

19. Sikora, A. G., Jaffarzad, N., Hailemichael, Y., Gelbard, A., Stonier, S. W., Schluns, K. S., Frasca, L., Lou, Y., Liu, C., Andersson, H. A., Hwu, P., and Overwijk, W. W. *IFN-alpha enhances peptide vaccine-induced CD8+ T cell numbers, effector function, and antitumor activity.* J Immunol. 2009. 182:7398-7407.

20. Adams, S., O'Neill, D. W., Nonaka, D., Hardin, E., Chiriboga, L., Siu, K., Cruz, C. M., Angiulli, A., Angiulli, F., Ritter, E., Holman, R. M., Shapiro, R. L., Berman, R. S., Berner, N., Shao, Y., Manches, O., Pan, L., Venhaus, R. R., Hoffman, E. W., Jungbluth, A., Gnjatic, S., Old, L., Pavlick, A. C., and Bhardwaj, N. *Immunization of malignant melanoma patients with full-length NY-ESO-1 protein using TLR7 agonist imiquimod as vaccine adjuvant.* J Immunol. 2008. 181:776-784.

21. Streilein, J. W. *Ocular immune privilege: therapeutic opportunities from an experiment of nature.* Nat.Rev.Immunol. 2003. 3:879-889.

22. Palmer, D. C., Chan, C. C., Gattinoni, L., Wrzesinski, C., Paulos, C. M., Hinrichs, C. S., Powell, D. J., Jr., Klebanoff, C. A., Finkelstein, S. E., Fariss, R. N., Yu, Z., Nussenblatt, R. B., Rosenberg, S. A., and Restifo, N. P. *Effective tumor treatment targeting a melanoma/melanocyte-associated antigen triggers severe ocular autoimmunity.* Proc.Natl.Acad.Sci.U.S.A 2008. 105:8061-8066.

23. Yeh, S., Karne, N. K., Kerkar, S. P., Heller, C. K., Palmer, D. C., Johnson, L. A., Li, Z., Bishop, R. J., Wong, W. T., Sherry, R. M., Yang, J. C., Dudley, M. E., Restifo, N. P., Rosenberg, S. A., and Nussenblatt, R. B. *Ocular and systemic autoimmunity after successful tumor-infiltrating lymphocyte immunotherapy for recurrent, metastatic melanoma.* Ophthalmology 2009. 116:981-989.

24. Ferrara, J. L. *Cytokine dysregulation as a mechanism of graft versus host disease.* Curr.Opin. Immunol. 1993. 5:794-799.

25. Grant, S. C., Lamb, W. R., Yonan, N., Hutchinson, I. V., and Brenchley, P. E. *Antithymocyte globulin preparations after heart transplantation. Cytokine responses in vivo and in vitro.* Transplantation 1995. 60:684-689.

26. Rockx, B., Baas, T., Zornetzer, G. A., Haagmans, B., Sheahan, T., Frieman, M., Dyer, M. D., Teal, T. H., Proll, S., van den, B. J., Baric, R., and Katze, M. G. *Early upregulation of acute respiratory distress syndrome-associated cytokines promotes lethal disease in an aged-mouse model of severe acute respiratory syndrome coronavirus infection.* J Virol. 2009. 83:7062-7074.

27. Suntharalingam, G., Perry, M. R., Ward, S., Brett, S. J., Castello-Cortes, A., Brunner, M. D., and Panoskaltsis, N. *Cytokine storm in a phase 1 trial of the anti-CD28 monoclonal antibody TGN1412.* N.Engl.J Med. 2006. 355:1018-1028.

28. Vonderheide, R. H., Flaherty, K. T., Khalil, M., Stumacher, M. S., Bajor, D. L., Hutnick, N. A., Sullivan, P., Mahany, J. J., Gallagher, M., Kramer, A., Green, S. J., O'Dwyer, P. J., Running, K. L., Huhn, R. D., and Antonia, S. J. *Clinical activity and immune modulation in cancer patients treated with CP-870,893, a novel CD40 agonist monoclonal antibody.* J Clin Oncol. 2007. 25:876-883.

29. Rosenberg, S. A., Yang, J. C., and Restifo, N. P. *Cancer immunotherapy: moving beyond current vaccines.* Nat.Med. 2004. 10:909-915.

30. Rosenberg, S. A. and Dudley, M. E. *Adoptive cell therapy for the treatment of patients with metastatic melanoma.* Curr.Opin.Immunol. 2009. 21:233-240.

8